1.B Damping of Ion-Acoustic Waves in the Presence of Electron-Ion Collisions

The study of ion-acoustic waves in plasmas has been the subject of considerable interest for the past 30 years.[1–7] Their damping rate plays an important role in establishing the threshold for the onset of stimulated Brillouin scattering, ion-temperature-gradient instability, current-driven ion-acoustic instability, and other drift-wave microinstabilities. In a collisionless plasma the waves are predominantly damped by electron Landau damping for $ZT_e >> T_i$, and by ion Landau damping for $ZT_e \sim T_i$ (where Z is the ionic charge and T is the temperature). The contribution of ion-ion (*i-i*) collisions to the damping is well understood, and the eigenfrequencies ω have been calculated for arbitrary values of $k\lambda_{ii}$ (where k is the wave number and λ_{ii} is the *i-i* mean free path), assuming isothermal electrons.[1] Kulsrud and Shen[2] were among the first to calculate the effect of introducing weak *e-i* collisions. They solved the linearized electron Fokker-Planck (FP) equation by expanding the distribution function about the collisionless result, and showed that for $k\lambda_{ei} >> 1$ (where λ_{ei} is the *e-i* mean free path) electron collisions give rise to a fractional *reduction* in the Landau damping rate of order $(m_i/Zm_e)/k\lambda_{ei}$. This curious "undamping" effect has been attributed to collisional disruption of the wave-particle resonance. It has since been confirmed by many authors using various models for the collision operator.[3–5] It has even been suggested that such an undamping effect, including possible instability, could be demonstrated experimentally.[5]

Here we present the first calculation of ion-acoustic wave damping based on an analytic solution of the electron FP and cold-ion fluid equations, for arbitrary *e-i* collisionality (omitting *e-e* collisions). This has been achieved by developing a reduced form of the FP equation with an (ω, k)-dependent *e-i* collision frequency. We show that the total damping rate can be accurately obtained by adding a collisional damping rate (arising from thermal diffusion) to a collisionally reduced Landau damping rate (arising from wave-particle interaction). However, despite the collisional disruption of Landau damping, collisional damping itself prevails so that there is no net undamping of the ion-acoustic wave. In fact, as *e-i* collisions are introduced, the damping rate γ rises monotonically above the collisionless Landau limit γ_L, reaches a peak at $k\lambda_{ei} \sim (Zm_e/m_i)^{1/2}$ (where the thermal-diffusion rate $\approx$ sound-transit rate), and then decreases to zero as $k\lambda_{ei} \rightarrow 0$, as predicted by fluid theory. The undamping effect predicted by previous authors is found to be an artifact of the method used in the derivation of the dispersion relation, which in most cases involved expanding the distribution function about the collisionless limit. Huang, Chen, and Hasegawa[4] realized the problem associated with this approach and adopted the approximate method of splitting the electron-distribution function into collisional and collisionless parts. However, by failing to correctly obtain the contribution from the highly collisional low-velocity part, they also predicted a reduction in the damping rate below γ_L. Dum,[6] who considered this problem in the context of strong turbulence, did indeed find that *e-i* collisions enhance the damping. However, his equations were not energy and momentum conserving, so that his results were only valid in the weakly collisional limit (i.e., $k\lambda_{ei} >> 1$). Recently, Bell[7] investigated the effect of e-i collisions on sound waves over the range $0 < k\lambda_{ei} < 1$ (i.e., for strong to intermediate collision strength) and found an enhancement in the damping above fluid-theory predictions for $k\lambda_{ei} > 0.01$. He attributed this enhancement to a reduction in the thermal conductivity below the classical Spitzer-Härm[8] (SH) value. In this article we also demonstrate a reduction in the thermal conductivity, and by extending the results to the collisionless limit ($k\lambda_{ei} >> 1$) we show that the effective thermal conductivity approaches the collisionless value calculated by Hammett and Perkins.[9]

We start by assuming a homogeneous plasma where the electrons collide elastically with cold-fluid ions only. Therefore, we neglect e-i energy exchange (since $m_e/m_i << 1$),[4] as well as i-i collisions. The effect of e-e collisions, which is expected to become important for low-Z plasmas, will be considered in a subsequent article. Adopting a perturbation of the electron-distribution function of the form

$$f(x,\mathbf{v},t) = F_0(v) + \sum_{l=0}^{\infty} f_l(v) P_l(\mu) \exp[-i(\omega t - kx)] \; , \tag{1}$$

where $\mu = v_x/v$ and $P_l(\mu)$ is the lth Legendre mode, the linearized electron FP equation (defined in the rest frame of the ions) becomes[10]

$$-i\omega f_0 + \frac{ikv}{3} f_1 - \frac{iku_i}{3} v \frac{\partial F_0}{\partial v} = 0 \; , \tag{2}$$

$$-i\omega f_1 + ikv f_0 + ikv \frac{2}{5} f_2 - \left(\frac{|e|E}{m_e} - i\omega u_i \right) \frac{\partial F_0}{\partial v} = -\nu_1 f_1 \; , \tag{3}$$

$$-i\omega f_2 + \frac{2}{3} ikv f_1 + \frac{3}{7} ikv f_3 - \frac{2}{3} iku_i v \frac{\partial F_0}{\partial v} = -\nu_2 f_2 \; , \tag{4}$$

and

$$-i\omega f_l + \frac{l}{2l-1} ikv f_{l-1} + \frac{l+1}{2l+3} ikv f_{l+1} = -\nu_l f_l \; , \tag{5}$$

for $l > 2$.

The ion velocity u_i and electric field E are first order in the perturbation and

$$F_0(v) = N_e \left(2\pi v_t^2 \right)^{-3/2} \exp\left(-v^2 / 2v_t^2 \right)$$

is an equilibrium Maxwellian, where N_e is the background electron number density and $v_t = \left(T_e / m_e \right)^{1/2}$ is the electron thermal velocity. The collision operators are given by $\nu_l(v) = \nu(v) l(l+1)/2$, where

$$\nu(v) = 4\pi N_e Z\left(e^2 / m_e\right)^2 \ln\Lambda / v^3$$

is the velocity-dependent *e-i* angular scattering collision frequency, *e* is the electron charge, and lnL is the Coulomb logarithm.

Substituting Eqs. (5) and (4) into (3) we obtain the following reduced form of the f_1 equation, which includes all contributions from $f_2, f_3, \ldots$,

$$ikvf_o - \left(\frac{|e|E}{m_e} - i\omega u_i + \frac{4k^2v^2}{15\nu_2^*}u_i\right)\frac{\partial F_o}{\partial v} = -\nu_1^* f_1 \,. \tag{3a}$$

This reduction has been accomplished by introducing an effective collision frequency $\nu_l^*(v,k,\omega) = \nu_l(v)\left[1 - i\omega / \nu_l(v)\right]H_l(v,k,\omega)$, where the effect of higher-order Legendre modes has been embodied in the continued fraction $H_l(v,k,\omega) = 1 + c_{l+1} / \left(1 + c_{l+2} / \ldots\right)$, with coefficients

$$c_l = 4k^2\lambda^2 / \left[\left(4l^2 - 1\right)\left(l^2 - 1\right)\left(1 - i\omega / \nu_l\right)\left(1 - i\omega / \nu_{l-1}\right)\right] \text{ and } \lambda \equiv v / \nu.$$

(This method of incorporating higher-order Legendre modes has also been successfully applied to the study of thermal filamentation.)[11] For the present analysis of low-frequency waves, setting $\omega = 0$ in ν^* (which leads to a purely real ν^*) has been found to have a negligible effect on the results. The continued fraction converges for all finite $k\lambda$, though a large number of terms are required as $k\lambda$ increases.

The linearized cold-ion continuity and momentum equations are

$$-i\omega n_i + ikN_i u_i = 0, \tag{6}$$

$$-i\omega N_i m_i u_i = ZN_i |e| E + R_{ie}, \tag{7}$$

where $R_{ie} = \left(4\pi m_e / 3\right)\int dv v^3 \nu f_1$ is the *i-e* momentum exchange rate, n_i is the perturbed ion number density, and N_i is its background value. Inserting Eqs. (2) and (3a) into (6) and (7) and assuming quasi-neutrality (i.e., $Zn_i \approx 4\pi\int dv v^2 f_o$) we obtain the dispersion relation

$$\left(\frac{\omega}{kc_s}\right)^2 = \frac{\left(1 + \eta J_4\right)^2}{J_7} - \eta\left(\eta J_1 + \frac{1}{3}\sqrt{\frac{2}{\pi}}\right), \tag{8}$$

where $c_s = (ZT_e/m_i)^{1/2}$ is the isothermal sound speed,

$$J_m = \sqrt{\frac{2}{\pi}}\int_0^\infty dV \frac{V^m \exp\left(-V^2/2\right)}{V^5 - 3\eta\left(1 - i\omega/\nu_1\right)H_1}, \tag{9}$$

$V = v / v_t$, $\eta = i(v_p / v_t)/(k\lambda_t)$ is a collisionality parameter, $v_p = \omega / k$ is the phase velocity, and $\lambda_t = \lambda(v_t)$ is the *e-i* scattering mean free path.

Equation (8) has been solved for $\omega = \omega_r - i\gamma$, and the normalized ion-acoustic damping rate γ/kc_s is plotted in Fig. 52.9 (solid curve) as a function of $k\lambda_{ei}$, for $A = 2Z$ [where A is the atomic mass and $\lambda_{ei} = 3T_e^2 / 4(2\pi)^{1/2} N_e^4 \ln\Lambda = 3(\pi/2)^{1/2}\lambda_t$]. Starting from the collisionless Landau limit $\gamma_L / kc_s = (\pi Z m_e / 8 m_i)^{1/2}$ (identified by the arrow on the right-hand side of the figure), we note that introducing weak collisions has the effect of enhancing the damping rate (by about 0.05% for $k\lambda_{ei} = 10^5$). This conclusion is in agreement with the results based on Dum's[6] model (shown by the dashed curve *a* of Fig. 52.9). However, since he neglected compressional heating [third term on the left-hand side of Eq. (2)] and the *i-e* momentum exchange rate [term R_{ie} in Eq. (7)], his dispersion relation becomes $\omega = kc_s / \sqrt{J_7}$, which is valid only for $k\lambda_{ei} >> 1$.

Kulsrud and Shen's[2] cold-ion damping rates are displayed as dashed curve *b* in Fig. 52.9. Their results, which imply a strong reduction in damping, followed by eventual wave growth ($\gamma < 0$), are typical of results based on small $1/k\lambda_{ei}$ expansions about the collisionless limit. Their physical explanation of undamping is that collisions disrupt the wave-particle resonance responsible for Landau damping. We find, however, that although collisions inhibit Landau damping, collisional damping itself prevails.

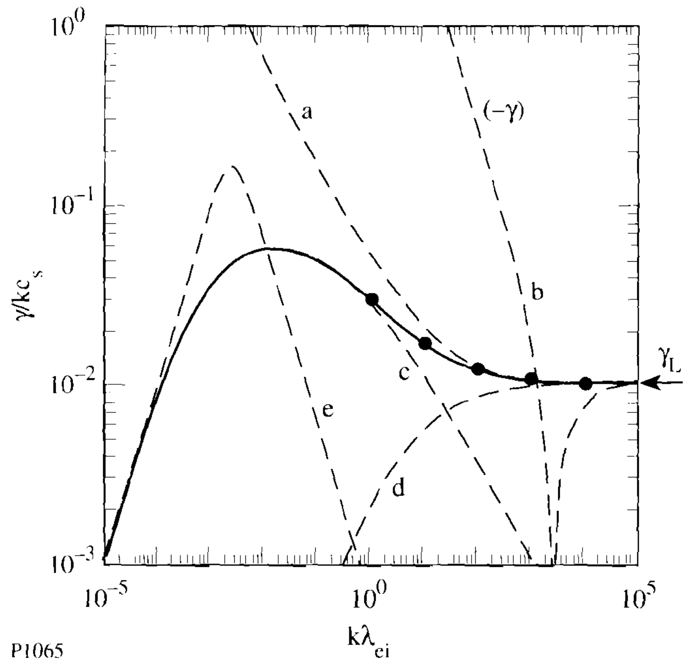

Fig. 52.9
Plots of damping rate of ion-acoustic waves γ/kc_s as a function of $k\lambda_{ei}$, where c_s is the isothermal sound speed, k is the perturbation wave number, and λ_{ei} is the electron-ion mean free path. The solid curve refers to the current FP results; dashed curves refer to models of (a) Dum, (b) Kulsrud and Shen, (c) Bell, (d) collisionally reduced Landau damping, and (e) fluid equations. The arrow on the right-hand side corresponds to the Landau damping rate γ_L/kc_s. Circles are obtained by adding curves *(c)* and *(d)*. Convergence required up to 400 terms in H_l for the largest value of $k\lambda_{ei}$.

Let us first consider the damping arising solely from collisions. We do this by solving the FP equation in the diffusive limit, which involves truncating the Legendre expansion [Eq. (1)] at $l = 1$ (or simply using $H_1 = 1$), and neglecting the $-i\omega f_1$ term in Eq. (3). Such an approach has been previously adopted by Bell[7] and gives rise to damping rates shown by the dashed curve *c* in Fig. 52.9. This type of damping results predominantly from electrons that diffuse across a distance k^{-1} in a time ω^{-1}. The velocity of these electrons can be estimated by setting $V^5 \sim 3|\eta|$ in the denominator of Eq. (9) and is found to be

$$v \sim v_c = v_t\left[9\left(\pi Z m_e / 2m_i\right)^{1/2} / k\lambda_{ei}\right]^{1/5}$$

To isolate the *collisionless* Landau-damping mechanism, which is dominated by electrons with velocities in phase with the wave (i.e., $v_x \sim v_p$), one would set $\nu = 0$. To include collisional disruption of the wave-particle interaction, we keep ν_l for all $l > 1$ yet set $\nu_1 = 0$. (The latter requirement ensures that there is no damping from thermal diffusion.) The corresponding damping rates, as shown in curve *d* in Fig. 52.9, fall below the collisionless Landau limit.

We find that the total damping rate can be obtained by adding the previously described "collisional damping" and "collisionally reduced, Landau-damping" rates. This is shown (as circles) in Fig. 52.9 over the range $1 < k\lambda_{ei} < 10^5$, where we find agreement with the full FP result to better than three significant figures. The reason for the successful superposition of both damping processes is that they originate from distinct regions in electron velocity space. This is illustrated by plotting contours in Figs. 52.10(a)–52.10(c) of the imaginary part of $f(v_x, v_\perp)$ (which is responsible for γ) as a function of v_x and

$$v_\perp = \left(v^2 - v_x^2\right)^{1/2}$$

at $k\lambda_{ei} = 10^5$. Figure 52.10(a) shows the result for collisional damping only. The dashed curve identifies electrons traveling with a velocity $v = v_c \approx 0.07 v_t$, which are the ones that can diffuse a distance $\sim k^{-1}$ in a time ω^{-1}. Since these dominate the collisional damping process, Im(f) has its maximum near $v = v_c$, with a peak in the direction of the heat flow. Figure 52.10(b) depicts the distribution for the collisionally reduced, Landau-damping mechanism, with $\nu_1 = 0$. The electron distribution is now concentrated along the dashed line $v_x = v_p$, where the electrons are in phase with the wave. However, unlike the classical collisionless case, where Im(f) is independent of $v_\perp$, we find that Im(f) is small near the origin. This is caused by strong collisional disruption of the wave-particle resonance, when the collision frequency $\nu(v) \propto 1/v^3$ becomes large. By comparing with the collisionless result (not shown), we also find a general broadening of the distribution about $v_x = v_p$. When both damping processes are operative, as shown in Fig. 52.10(c), one can still clearly identify the distinctive features of each.

Let us now consider the collisional regime $k\lambda_{ei} < 1$. Dashed curve *e* in Fig. 52.9 shows the classical damping rate derived from the fluid equations, neglecting

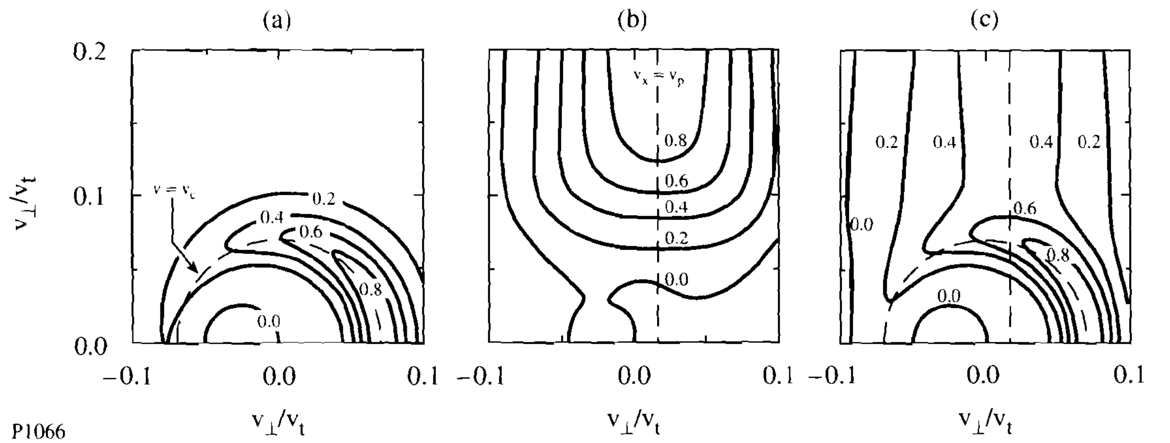

Fig. 52.10
Normalized contour plots of the perturbed distribution function Im(f) (in intervals of 0.2) as a function of v_x and $v_\perp$, for (a) collisional damping, (b) collisionally reduced Landau damping, and (c) full damping (for $k\lambda_{ei} = 10^5$).

electron viscosity.[12] As expected, when $k\lambda_{ei} \to 0$, fluid and kinetic results are in agreement. In the fluid limit, the maximum γ is found to occur when the ratio of the thermal-diffusion rate to the sound-transit rate is of order unity, i.e., $2k^2\kappa_{SH}/3n_ekc_s \sim k\lambda_{ei}(m_i/Zm_e)^{1/2} \sim 1$, where κ_{SH} is the SH thermal conductivity. When $k\lambda_{ei}(m_i/Zm_e)^{1/2} > 1$, electron kinetic effects start to dominate and fluid theory breaks down. Associated with this breakdown is a reduction in the effective thermal conductivity $\kappa \equiv -q/ikT_{FP}$ [where $q = (2\pi m_e/3)\int dv v^5 f_1$, and $T_{FP} = (4\pi m_e/N_e)\int dv(v^4/3 - v^2 v_t^2)f_0$] relative to κ_{SH}, as shown by the solid curve in Fig. 52.11(a). This heat flow inhibition, first pointed out by Bell[7] [dashed curve a in Fig. 52.11(a)], is a consequence of the decoupling between the relatively collisionless heat-carrying electrons and the bulk thermal-electron population. In the $k\lambda_{ei} >> 1$ limit our result agrees with the heat-flow coefficient obtained by Hammett and Perkins[9] [dashed curve b in Fig. 52.11(a)] for a collisionless plasma. It should be noted that the effective conductivity is actually complex over a wide range of $k\lambda_{ei}$, as shown by the phase plot of κ in Fig. 52.11(b).

In summary, we have developed a simplified form of the FP equation that is valid for arbitrary e-i collisionality, through the introduction of a generalized collision frequency $\nu^*(v,k,\omega)$. We have demonstrated that the effective damping of a sound wave can be treated as a linear combination of a purely collisional damping and a collisionally reduced Landau damping. In contrast to results in several published works, the introduction of e-i collisions increases the damping above the collisionless Landau value.

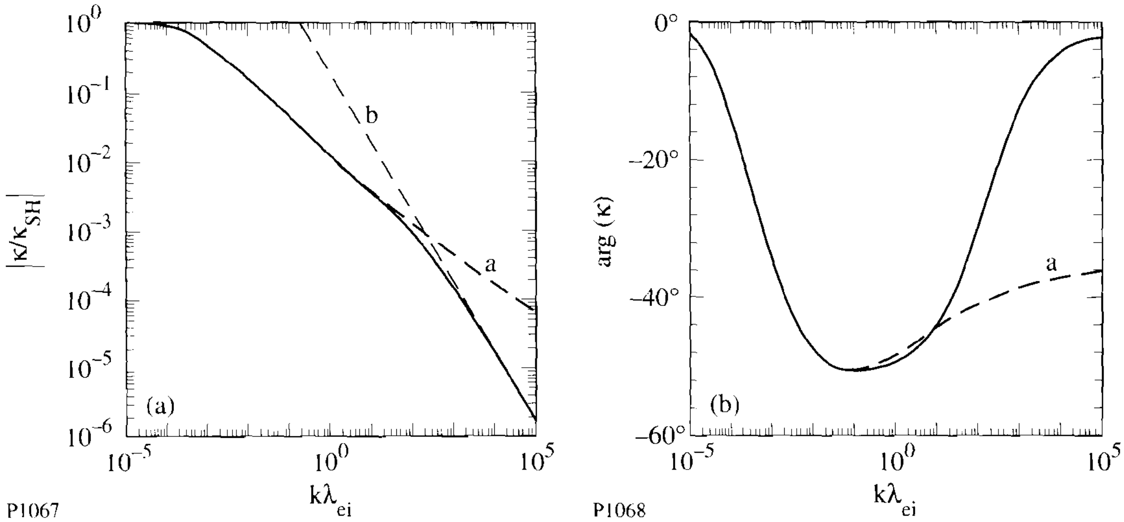

Fig. 52.11
Plots of (a) $|\kappa/\kappa_{SH}|$ and (b) arg(κ) as a function of $k\lambda_{ei}$, where κ and κ_{SH} are the effective and Spitzer-Härm thermal conductivities, respectively. The solid curve refers to the current FP results; dashed curves refer to models of (a) Bell and (b) Hammett and Perkins.

ACKNOWLEDGMENT

This work was supported by the U.S. Department of Energy Office of Inertial Confinement Fusion under agreement No. DE-FC03-85DP40200 and by the Laser Fusion Feasibility Project at the Laboratory for Laser Energetics, which is sponsored by the New York State Energy Research and Development Authority and the University of Rochester.

REFERENCES

1. D. Bhadra and R. K. Varma, Phys. Fluids **7**, 1091 (1964); M. Ono and R. M. Kulsrud, Phys. Fluids **18**, 1287 (1975); C. J. Randall, Phys. Fluids **25**, 2231 (1982).
2. R. M. Kulsrud and C. S. Shen, Phys. Fluids **9**, 177 (1966).
3. B. Buti, Phys. Rev. **165**, 195 (1968); R. S. B. Ong and M. Y. Yu, J. Plasma Phys. **3**, 425 (1969); R. J. Stéfant, Phys. Fluids **14**, 2245 (1971).
4. T.-Y. Huang, L. Chen, and A. Hasegawa, Phys. Fluids **17**, 1744 (1974). The proper solution of their Eq. (15), to lowest order in $1/D(v)$, is the result they give in Eq. (23) plus an added ψ-independent term $-\alpha F_e{}^o v/6Dv_\varphi$. The resultant density perturbation, from their low-velocity region, no longer vanishes.
5. J. R. Jasperse and B. Basu, Phys. Rev. Lett. **58**, 1423 (1987); B. Basu and J. R. Jasperse, Phys. Rev. A **38**, 3785 (1988).
6. C. T. Dum, Phys. Rev. Lett. **35**, 947 (1975).
7. A. R. Bell, Phys. Fluids **26**, 279 (1983).
8. L. Spitzer and R. Härm, Phys. Rev. **89**, 977 (1953).

9. G. W. Hammett and F. W. Perkins, Phys. Rev. Lett. **64**, 3019 (1990).

10. I. P. Shkarofsky, T. W. Johnston, and M. P. Bachynski, *The Particle Kinetics of Plasmas* (Addison-Wesley, London, 1966); T. W. Johnston, J. Math. Phys. **7**, 1453 (1966).

11. E. M. Epperlein and R. W. Short, Phys. Fluids B **4**, 2211 (1992).

12. P. M. Morse and H. Feshbach, *Methods of Theoretical Physics* (McGraw-Hill, New York, 1953), Part I, p. 268.